# A new analytical model for predicting SWCNT band-gap from geometrical properties

Karim El Shabrawy *(IEEE Student member)*, Koushik Maharatna *(IEEE member)*, Darren M Bagnall, Bashir M Al-Hashimi

***Abstract*—In the following paper we present a complete analytical model that predicts the band-gap ($E_g$) of Single-Walled Carbon nanotubes (SWCNTs) directly from their diameter ($d$) and chiral angle ($\theta$). The proposed analytical model is based on two mathematical expressions that have been derived by curve-fitting the outcome generated from the third-nearest-neighbor Tight-Binding (TB) method in conjunction with the zone-folding technique. Tests performed on the model demonstrated that 82% of a set of both metallic and semiconducting CNTs were accurately distinguished. In addition, the maximum band-gap error recorded for the semiconducting tubes was 10%. The model was also verified against previously published experimental data where 17 out of 21 tubes were correctly predicted. Finally, it is shown that the proposed model computes $E_g$ with a speed that is $10^5$ times faster compared to the third-nearest-neighbor TB method with zone-folding. The outcome of this work offers a fast and accurate technique for engineers who are seeking to simulate CNT based devices and want to ascertain the CNT's electronic properties with respect to the geometrical variation manifested in their synthesis process.**

***Index Terms*—Single-Walled Carbon Nanotube (SWCNT) electronic properties, third-nearest-neighbor tight-binding model, Energy band gap, semiconductor device modeling.**

## I. Introduction

CARBON NANOTUBES are anticipated to play a central role in realizing nanoelectronic devices for future Integrated Circuits (ICs) as well as other applications [1]. They can remarkably exhibit semiconducting ($E_g > 0$) or metallic ($E_g = 0$) behavior depending on their geometrical structure, which includes the diameter ($d$) and chirality (the direction in which the carbon sheet is rolled-$\theta$) [2]. Even though the diameter can be controlled to a limited extent (i.e. by specifying the catalyst particle size for a given CNT synthesis process [1]), the chirality cannot and hence the conductive properties of CNTs can vary immensely within a single produced batch. Engineers must take account of this variation in their CNT based device models in order to reproduce *I-V* characteristics that closely reflect experimental measurements.

Previous studies have confirmed the sensitivity of the CNT's band-gap to both $d$ and $\theta$, where several theoretical and analytical models have been established to simulate their electronic band-structure [3-9]. Amongst the commonly used band models are the nearest-neighbor and third-nearest-neighbor Tight-Binding (TB) approximation with zone-folding [3-6, 9], the Extended Hückel Theoretical (EHT) technique [7] and first-principle *ab-initio* calculations [8, 9]. Although very accurate, the listed models are computationally expensive and possess a time complexity that increases with the size of the nanotube. For applications that require simultaneous simulation of millions of dissimilar CNT-devices these models would be very difficult to utilize in a timely manner.

Analytical models such as those mentioned in [10, 11] were formed by experimentally probing semiconducting CNTs to identify their geometric structure and measure their corresponding electrical output characteristics. In turn, results are plotted and curves extrapolated to capture the CNT band-gap [8]. These models merely apply to semiconducting tubes and consequently only 2/3$^{rd}$ of the nanotube's band-gap can be predicted [3]. Moreover, chirality is not considered in calculating $E_g$ undermining the model's accuracy [12]. Although the analytical model proposed in [12] does consider chirality, they presume that the type of CNT being dealt with is already known.

Herein, we propose an analytical model with a time complexity that's independent of the size of the nanotube and simply consists of two mathematical equations that directly determine the CNT band-gap ($E_g$). Given only $d$ and $\theta$, the first expression distinguishes whether the SWCNT is semiconducting or metallic. This formula was tested against results produced using the third-nearest-neighbor TB method with zone-folding where a random set of both metallic and semiconducting tubes were analyzed. From a set of 1479 SWCNTs 82% were correctly differentiated. In the case that the tube is revealed to be semiconducting another expression is evaluated to define $E_g$. Similarly, the second expression was assessed against results delivered by the third-nearest-neighbor TB method for all semiconducting tubes and the maximum band-gap error achieved was 10%. In the final section of this paper we show that the model is in agreement with two separate sources of experimental data. Additionally, runtime improvements over band-structure calculations are presented.

Paper submitted on 29/02/08 for review. The authors are with the School of Electronics and Computer Science (ECS), Southampton University, Southampton, UK, SO17 1BJ (e-mail: kes06r@ecs.soton.ac.uk).

## II. SWCNT ELECTRONIC STRUCTURE

A Single-Walled Carbon Nanotube (SWCNT) is a self-assembled hollow cylinder constructed from a rolled-up sheet of graphene [9]. The tube can be uniquely defined by a roll-up vector known as the chiral vector, $\mathbf{C_h}$, which can be expressed in terms of the primitive unit vectors $\mathbf{a_1}$ and $\mathbf{a_2}$ of the graphene lattice [3]:

$$\mathbf{C_h} = m\mathbf{a_1} + n\mathbf{a_2} \tag{1}$$

where $m$ and $n$ are integers that are specific to a $(m,n)$ CNT [3]. The magnitude of $\mathbf{C_h}$ corresponds to the circumference around the nanotube. This can be used to determine the diameter ($d$) as denoted by (2).

$$d = \frac{\sqrt{3}}{\pi} a_{cc} \sqrt{m^2 + nm + n^2} \tag{2}$$

In (2) the constant $a_{cc}$ (0.142nm) represents the nearest-neighbor C-C distance [11]. The chiral angle ($\theta$) is defined as the angle between $\mathbf{C_h}$ and $\mathbf{a_1}$, which can be expressed as [1]:

$$\theta = \tan^{-1}\left(\frac{\sqrt{3}n}{2m+n}\right) \tag{3}$$

Typically, to identify the electronic properties of a SWCNT the dispersion relation of graphene is obtained using a TB approach. Next, the Born-von Karman periodic boundary conditions are imposed along the circumferential direction slicing the 2D band-structure of graphene into 1D sub-bands [9]. If one of these slices intersects with a high symmetry K point in the Brillouin zone of graphene (where conduction and valence band touch at the Fermi-level) the nanotube can be considered metallic [13]. Otherwise, the nanotube is semiconducting with a finite $E_g$. According to the choice of $n$ and $m$, each CNT will have a different electronic band-structure. This is known as the zone-folding technique and is sufficient in approximating the CNT band-gap for a tube with any chirality and diameter.

However, in [6] it was shown that the nearest-neighbor TB approximation does not accurately reproduce the graphene band-structure compared to *ab initio* calculations. Instead, it was revealed that the third-neighbor TB approach yielded better fitting results along the high-symmetry points of the Brillouin zone and that the CNT band-structure improves by including more distant neighbors [6].

A simulation was run using the third-neighbor TB approach with fitting parameters extracted from [6] in conjunction with the zone-folding technique to calculate the band-gap for a set of SWCNTs. These tubes were characterized by all possible chiralities, $0^0$-$30^0$, and diameters ranging between 0.35nm-2.55nm. Fig. 1 shows the calculated $E_g$ for various $\theta$ and $d$.

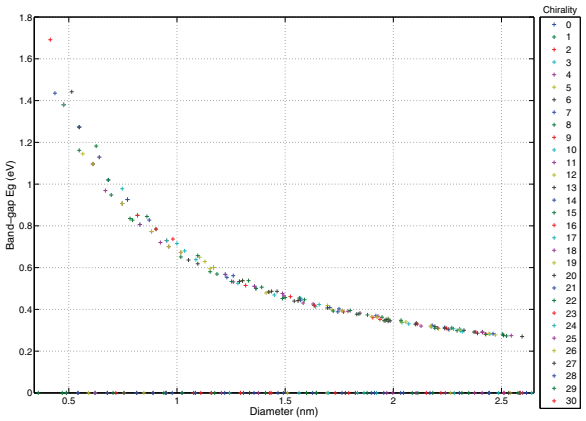


Fig. 1 SWCNT band-gap ($E_g$) for different geometrical properties, $d$ and $\theta$. CNTs with different chirality are illustrated by separate colour shading.

## III. ANALYTICAL APPROACH TO DISTINGUISHING SWCNTS

The geometric variables ($d$, $\theta$) that produced a zero band-gap were collected separately and plotted as data points shown in Fig. 2.

To establish an expression that will enable us to predict these data points a relationship between $d$ and $\theta$ was initially derived. By rearranging (3) to get $m$ in terms of $n$ and $\theta$, then substituting into (2) gives the following:

$$d = \frac{3a_{cc}}{2\pi}\frac{n}{\sin\theta} \tag{4}$$

If we assume that the sine function of (4) can be approximated by a first-degree polynomial ($b\theta+c$) over the interval $0^0 \leq \theta \leq 30^0$ then it can be inferred that the diameter $d$ is inversely proportional to $b\theta+c$. By examining the data points in Fig. 2 it could be speculated that if several distinct curves were to be fitted over the points then they would all share the same asymptote at $\theta=30^0$. Thus, $b$ can be expressed in terms of $c$ as $b=-c/30$, which now leaves us with only one unknown variable; $c$.

By limiting our focus to the zigzag tubes ($\theta=0^0$) a pattern can be recognized in the tube diameters that offer a zero band-gap. These diameters include: 0.4697, 0.7046, 0.9395, 1.1743…, which can be expressed as an arithmetic progression yielding a sequence of values for $c$. Combining the abovementioned results to form an expression for the zero band-gap data points gives:

$$d(\theta,k) = \left(\frac{2.1289}{(0.5(k-2)+1)}\left(\frac{-1}{30}\theta+1\right)\right)^{-1} \tag{5}$$

where $k$=1,2,3,…N. N is set by the maximum diameter size ($d_{max}$) chosen for a zigzag CNT and is given by N=2((2.1289$d_{max}$)-1)+2. In our case N is selected to be 10

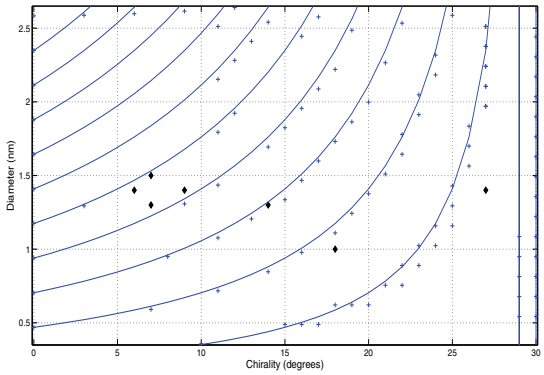


Fig. 2. Zero band-gap ($E_g$) points for different geometrical properties, $d$ and $\theta$. Those depicted by + are metallic CNTs generated by running the third-neighbor TB approach with the zone-folding technique. Those depicted by ♦ are metallic CNTs that were experimentally measured in [11]. ── Curves represent equation (5) for $k$=1-10.

since $d_{max}$=2.55nm. As shown in Fig. 2 the expression given by (5) for k=1,2,..10 supplies 10 curves that fit reasonably well with the data points. However, (5) fails to predict the Armchair tubes ($\theta$=30$^0$), which exhibit a zero $E_g$ for all diameters [1].

To predict the zero band-gap tubes a function can be formulated that assumes a value of zero only when either $\theta$=30$^0$ or the diameter lies on one or more of the curves approximated by (5) for a given geometry. Mathematically, this can be expressed as:

$$f(\theta,d)=(\theta-30)\prod_{k=1}^{N}\left(\frac{4.2578d}{k}\left(\frac{-1}{30}\theta+1\right)-1\right) \qquad (6)$$

Equation (6) was tested by sourcing the geometrical properties of 1479 metallic and semiconducting CNTs. The results for $f(\theta,d)$ are depicted in Fig. 3.

Upper and lower tolerance margins for $f(\theta,d)$ were added to maximize the identification of metallic tubes whilst minimizing the misdetection of semiconducting tubes as

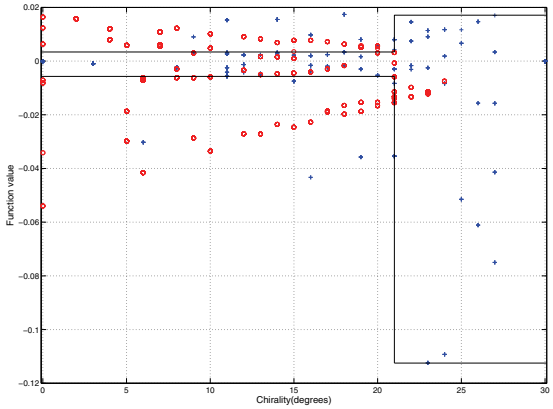


Fig. 3. Values of $f(\theta,d)$ for 1479 metallic (+) and semiconducting (o) SWCNTs plotted against chirality, $\theta$. Tolerance margins are added as illustrated by the black lines to optimize the distinguishing accuracy.

metallic. The margins of 0.0034 and -0.0057 were set, respectively, for tubes with chirality lower than 21$^0$. Similarly, above 21$^0$ the upper and lower margins were set to 0.0171 and -0.1125, respectively. This enabled us to distinguish metallic from semiconducting tubes with an 82% accuracy.

## IV. Analytical Approach for Calculating Semiconducting CNT Band-Gap

From Fig. 1 we observe that for all semiconducting SWCNT's the dependence of $E_g$ on diameter is inversely proportional. This reinforces the $1/d$ relationship derived in [1, 5, 8-12, 14]. However, all these sources differ on an additional factor that is used during the calculation of a semiconducting CNT band-gap; the overlap energy $\gamma_0$. $\gamma_0$ is a constant that has been debated to be in the range 2.45eV-2.90eV and no agreed value has ever emerged [12]. In [12] it was mentioned that the reason for the resulting discrepancy in $\gamma_0$ is due to the fact that chirality is neglected when interpreting the band-gap for different diameters. Thus, here we have collected the band-gap produced for all semiconducting tubes and plotted $E_g$ with respect to $d$ for every $\theta$. Subsequently, a curve fitting tool is used to establish a relationship between all these parameters.

Fig. 4 shows the resulting optimum curve and is given by:

$$E_g=10.2\frac{3a_{cc}}{2\pi d}=\frac{0.69}{d} \qquad (7)$$

From (7) it can be confirmed that $E_g$ is proportional to $1/d$ and the constant of proportionality is independent of $\theta$. In fact, if the overlap energy is calculated from (7) we get 2.44eV, which is similar to the value generated by experiment (2.45eV) in [10]. This offers a consistency check for our approach.

When the geometric properties of all semiconducting CNTs were sourced into (7) and the $E_g$ error was calculated compared to the third-neighbor TB approach with zone folding the maximum error recorded was only 10%.

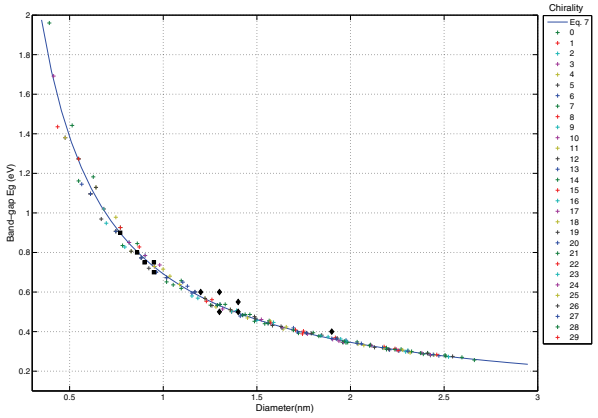


Fig. 4. Semiconducting band-gap vs. diameter for all θ. CNT's with different chirality are illustrated by a separate colour shading. + represents results obtained using the third-nearest-neighbor TB approach with the zone-folding technique. ― is the fitting curve given by equation (7). ♦ depicts exp. measurements made in [11]. ■ depicts exp. measurements made in [10].

978-1-4244-1811-4/08/$25.00 © 2008 IEEE

| Tube no# | $\theta$(°) | $d$(nm) | Exp. $E_g$ (eV) | Proposed model $E_g$ (eV) | $E_g$ % error for semi. CNTs | TB+ZF $E_g$ (eV) | TB + ZF runtime (ms) | Proposed model runtime (ms) | Speed increase |
|---|---|---|---|---|---|---|---|---|---|
| 1 | 25 | 1.4 | 0.55 | 0 | N/A | 0 | 12001.663 | 0.075 | 160022.2 |
| 2 | 4 | 1.4 | 0.6 | 0 | N/A | 0.736 | 18448.638 | 0.096 | 192173.3 |
| 3 | 7 | 2 | 0.5 | 0.3458 | 30.84 | 0.308 | 45429.711 | 0.064 | 709839.2 |
| 4 | - | 1.3 | 0.65 | 0.532 | 18.15 | 0.534 | 31572.849 | 0.096 | 328883.8 |
| 5 | 30 | 1.3 | 0 | 0 | 0 | 0 | 1259.96 | 0.089 | 14156.9 |
| 6 | 7 | 1.3 | 0 | 0 | 0 | 0.65 | 22912.701 | 0.096 | 238673.9 |
| 7 | 14 | 1.3 | 0 | 0 | 0 | 0.4788 | 7473.967 | 0.082 | 91145.9 |
| 8 | 16 | 1.2 | 0.6 | 0.5763 | 3.95 | 0.5613 | 29556.109 | 0.075 | 394081.5 |
| 9 | 6 | 1.3 | 0.6 | 0.532 | 11.33 | 0.532 | 29660.008 | 0.064 | 463437.6 |
| 10 | 29 | 1.3 | 0.5 | 0.532 | 6.4 | 0.534 | 30876.521 | 0.099 | 311884.1 |
| 11 | 16 | 1.9 | 0.4 | 0.364 | 9 | 0 | 6068.544 | 0.096 | 63214 |
| 12 | 18 | 1 | 0 | 0.6916 | N/A | 0 | 7757.727 | 0.124 | 62562.3 |
| 13 | 9 | 1.4 | 0 | 0 | 0 | 0 | 10805.108 | 0.074 | 146014.9 |
| 14 | 7 | 1.5 | 0 | 0 | 0 | 0.418 | 115784.15 | 0.077 | 1503690. |
| 15 | 27 | 1.4 | 0 | 0.494 | N/A | 0.511 | 74317.13 | 0.102 | 728599.3 |
| 16 | 6 | 1.4 | 0 | 0 | 0 | 0.532 | 63774.201 | 0.104 | 613213.5 |
| 17 | - | 0.77 | 0.9 | 0.8981 | 0.21 | 0.907 | 22435.63 | 0.096 | 233704.5 |
| 18 | - | 0.86 | 0.8 | 0.8041 | 0.5125 | 0.773 | 31664.675 | 0.098 | 323108.9 |
| 19 | - | 0.9 | 0.75 | 0.7684 | 2.45 | 0.773 | 31543.438 | 0.084 | 375517.1 |
| 20 | 11 | 0.95 | 0.75 | 0.728 | 2.93 | 0 | 5486.623 | 0.101 | 54323 |
| 21 | 11.7 | 0.95 | 0.7 | 0.728 | 4 | 0.716 | 40513.979 | 0.105 | 385847.4 |

Table I. Comparison between experimentally measured $E_g$ and proposed model $E_g$ for a set of 21 SWCNTs with various geometric properties. The runtimes for the third-neighbor TB approach with zone-folding (TB+ZF) and the proposed model are also compared.

## V. Comparison with Experimental Results

In order to verify the proposed analytical model comparisons are made with respect to two sources that generate experimental results using different techniques.

In [11] Scanning Tunneling Spectroscopy (STS) is used to examine the electronic properties as a function of $d$ and $\theta$ for a set of SWCNTs. The measurements obtained are depicted in Fig. 2 and Fig. 4 as well as in Table I (tube no$^{\#}$ 1-16). In [10] Scanning Tunneling Microscopy (STM) characterization of the SWCNTs was undertaken and the band-gap of 5 nanotubes were extracted and recorded as shown in Table I (tube no$^{\#}$ 17-21) as well as in Fig. 4.

From Table I it can be deduced that out of a total of 21 SWCNTs 17 were correctly distinguished. Furthermore, we can establish that our band-gap results are more consistent with STM measurements compared to STS measurements. For the CNTs shown in Table I we demonstrate that the proposed model computes $E_g$ on average 352099.7~$10^5$ times faster than the third-neighbor TB approach with zone-folding.

## VI. Conclusion

An analytical model to calculate the band-gap of SWCNTs directly from their geometrical structure is proposed. Tests compared to the third-nearest-neighbor TB approach with zone folding showed that out of a random set of metallic and semiconducting CNTs, 82% were distinguished accurately. Moreover, for semiconducting CNTs a maximum $E_g$ error of 10% was achieved. When compared to two sources of experimental data the proposed model is able to distinguish 17 out of 21 SWCNTs correctly. Finally, we verify that the analytical model computes $E_g$ with a speed that is of the order of $10^5$ times greater than the TB approach with zone folding.

## References


[1] M. S. Dresselhaus, R. Saito, and A. Jorio, "Semiconducting Carbon Nanotubes," *Proceedings of ICPS* vol. 27, 2004

[2] M. Terrones, "Science and Technology of the Twenty-First Century: Synthesis, Properties, and Applications of Carbon Nanotubes," *Annual Review of Materials Research,* vol. 33(1), 2003.

[3] R. Saito, M. Fujita, G. Dresselhaus, and M. S. Dresselhaus, "Electronic structure of chiral graphene tubules," *Appl. Phys. Lett.* , vol. 60, 1992.

[4] N. Hamada, S. Sawada, and A. Oshiyama, "New one-dimensional conductors: Graphitic microtubules " *Phys. Rev. Lett.,* vol. 68, pp. 1579 - 1581, 1992.

[5] R. Saito, M. S. Dresselhaus, and G. Dresselhaus, *Physical Properties of Carbon Nanotubes*: Imperial College Press, 1998.

[6] S. Reich, J. Maultzsch, C. Thomsen, and P. Ordejón, "Tight-binding description of graphene," *Physical Review B,* vol. 66, p. 035412, 2002.

[7] D. Kienle, J.I. Cerda, and A. W. Ghosh, "Extended Hückel theory for bandstructure, chemistry and transport : I. Carbon Nanotubes," *J. Appl. Phys.,* vol. 100, p. 043714., 2006.

[8] O. Gülseren, T. Yildirim, and S. Ciraci, "Systematic ab initio study of curvature effects in carbon nanotubes," *Physical Review B,* vol. 65, p. 153405, 2002.

[9] J. W. Mintmire and C. T. White, "Electronic and Structural properties of Carbon nanotubes," *Carbon,* vol. 33 pp. 893-902 1995.

[10] Teri Wang Odom, Jin-Lin Huang, Philip Kim, and C. M. Lieber, "Atomic structure and electronic properties of single-walled carbon nanotubes," *Nature,* vol. 391, pp. 62-64, 1998.

[11] Jeroen W. G. Wildoer, Liesbeth C. Venema, Andrew G. Rinzler, Richard E. Smalley, and C. Dekker, "Electronic Structure of atomically resolved carbon nanotubes," *Nature,* vol. 391, pp. 59-62, 1998.

[12] J. W. Ding, X. H. Yan, and J. X. Cao, "Analytical relation of band gaps to both chirality and diameter of single-wall carbon nanotubes," *Physical Review B,* vol. 66, 2002.

[13] J. R. Hauptmann, "Spin-Transport in Carbon Nanotubes," in *Faculty of Science*. vol. Master of Science: University of Copenhagen, 2003.

[14] C. L. Kane and E. J. Mele, "Size, Shape, and Low Energy Electronic Structure of Carbon Nanotubes," *Phys. Rev. Lett.,* vol. 78, 1997.


978-1-4244-1811-4/08/$25.00 © 2008 IEEE